



# Study of Stickiness Perception of Fabrics Based on Friction and ERP Method

Xingxing Fang<sup>1</sup> · Wei Tang<sup>1</sup> · Chaoquan Tang<sup>1</sup> · Meimei Zhang<sup>1</sup> · Yuxing Peng<sup>1</sup>

Received: 19 October 2022 / Accepted: 23 January 2023 / Published online: 6 February 2023  
© The Author(s), under exclusive licence to Springer Science+Business Media, LLC, part of Springer Nature 2023

## Abstract

Sweats within the fabric–skin interface increase friction, cause stickiness perception, and facilitate wearing discomfort. To study the stickiness perception of wet fabrics, subjective assessment, skin friction, and neurophysiological response of the brain were systematically studied. Four fabrics that are commonly used as summer clothing were chosen for the tactile stimulus samples. Different wetness levels were designed by changing the sweat absorption amount. The results showed that the adhesive friction played a dominant role when the skin contacted the dry fabrics. The features of the friction coefficient  $\mu$ , multiple fractal spectrum width, and P300 amplitude had strong correlations with the perceived stickiness of fabrics. Under dry and moist conditions, the surface roughness and water absorption capacity of fabric were the dominant factors that influenced the friction, vibration, and stickiness perception of fabrics. The parietal lobe and occipital lobe were positively activated and involved in the stickiness perceptions of fabric. Fabrics with low water absorption capacity and high  $\mu$  tended to excite a high P300 amplitude and large activated brain area. The mechanical stimulation of the tactile receptor is associated with the brain's cognition during stickiness perception. This study is meaningful for understanding the frictional behavior between fabric and skin surface and the cognitive mechanism in the stickiness perception of fabrics to reduce friction and improve wear comfort. It is also helpful in the evaluation of tactile stimulation of fabrics.

**Keywords** Stickiness perception · Friction · Event-related potentials · Fabric

## 1 Introduction

Sweating is experienced in everyday life, especially in hot and humid environments. Due to the presence of sweat, clothes may stick to our skin and cause discomfort, which is often referred to as a sensation of stickiness [1, 2]. The stickiness and moisture sensations are the most important factors contributing to the discomfort of fabrics during wear. Meanwhile, skin injuries such as blisters, decubitus, and abrasions are greatly influenced by the friction and moisture between human skin and fabrics [3]. Therefore, it is crucial to research the frictional behavior between fabric and skin surface as well as the related stickiness perception to reduce the friction and improve the wear comfort.

Stickiness, which can stick to any surface when contacted, is connected to the friction that occurs when one surface

slides over another. When sliding a fabric over our skin, the deformation, vibration, and friction of the skin surface induced by properties of the fabric stimulate sensory receptors in the skin. Sensory receptors detect and transform these mechanical stimulations into nerve action potentials. Then, nerve action potentials are transmitted to the corresponding sensing area of the cerebral cortex through the afferent nerve, spinal cord, and brain stem. Finally, a sensation of stickiness is developed in the somatosensory cortex, and sensorial judgments of stickiness are reported by the subject [4–6]. Therefore, the tactile sensation of fabric is derived from the vibrations and friction of skin and is formed in the somatosensory cortex [5, 6]. The study of stickiness perception of fabrics involves tribology and neurophysiology [7, 8]. Currently, many studies have focused on the influence of moisture on skin friction against different textiles. Linear, power law, exponential, and bell-shaped relationships between skin hydration and friction have been reported in research on the qualitative relationship between skin moisture and friction [9]. To explain the increase in the friction coefficient under various moist skin conditions, physical

✉ Wei Tang  
tangwei@cumt.edu.cn

<sup>1</sup> School of Mechatronic Engineering, China University of Mining and Technology, Xuzhou 221116, Jiangsu, China

friction mechanisms, such as water absorption, viscous shearing, and capillary adhesion, have been studied [10]. Some studies also involved the correlation of skin friction and stickiness perception of wet fabrics. According to Jiang et al.'s investigation, stickiness sensations under friction and adhesion–separation modes were significantly negatively correlated with the water absorption capacity [11]. A study conducted by Zhang et al. [12] showed that the type of fabric, water content, and friction velocity have a significant influence on skin perceptual wetness and a stronger wetness sensation was perceived when the frictional coefficient and friction velocity were low.

Compared with the friction study related to stickiness perception, the cognitive mechanisms of the brain associated with stickiness perception have received little attention and are not well understood. Due to high temporal resolution and low cost, EEG (electroencephalograph) and ERP (event-related potentials) technology can be utilized to evaluate cognitive functions and brain ability [13–15]. Many studies have proven that ERP can be used to isolate and explore the brain activity related to the tactile exploration of natural textures [13, 16, 17]. According to some studies, friction and vibration experienced in tactile perception might cause neuronal entrainment at the cerebral level such as peak latency and amplitude of earlier somatosensory evoked potential components P100 and P200 of ERP signals and typical endogenous component P300 of ERP signals [18–20].

Friction is an important stimulating factor of tactile perception when touching fabrics and brain activities in response to a fabric stimulus are critical in understanding the cognitive mechanism of tactile perception. This investigation systematically studied the stickiness perception of fabrics based on subjective assessment, surface friction and vibration, and the neurophysiological response of the brain.

Different wetness levels of fabric were designed by changing the sweat absorption amount. The fabric features that influenced the friction coefficients, vibration, and stickiness perceptions were analyzed and the related friction mechanism was discussed under different wetness levels of various fabrics. To identify the brain regions and neural activity related to stickiness perception, the ERP method was used to measure the event-related voltage changes in the brain response when they felt various fabrics under different wetness levels. Meanwhile, to quantify the stickiness perceptions of fabrics, the features extracted from the friction, vibration, and ERP signals were correlated with the subjective stickiness sensation rated by questionnaires. This study contributes to the understanding of frictional behavior between fabric and skin surface and the cognitive mechanism of stickiness sensation. Furthermore, it provides an evaluation method for the stickiness perception of fabrics under different wetness levels and is meaningful for applications, such as intimate apparel, sportswear, and healthcare products.

## 2 Experimental Details

### 2.1 Samples

Linen, cotton, polyester, and silk fabric, which are commonly used as summer clothing, were chosen for the tactile stimulus samples. The size of the samples was 60 × 60 mm. The microscopic images of the surfaces of the fabric samples are shown in Fig. 1, and their structure, component, warp-weft density, and surface roughness are shown in Table 1. The surface roughness of the fabrics was measured using an Olympus DSX 1000 digital microscope (Olympus, Tokyo, Japan).

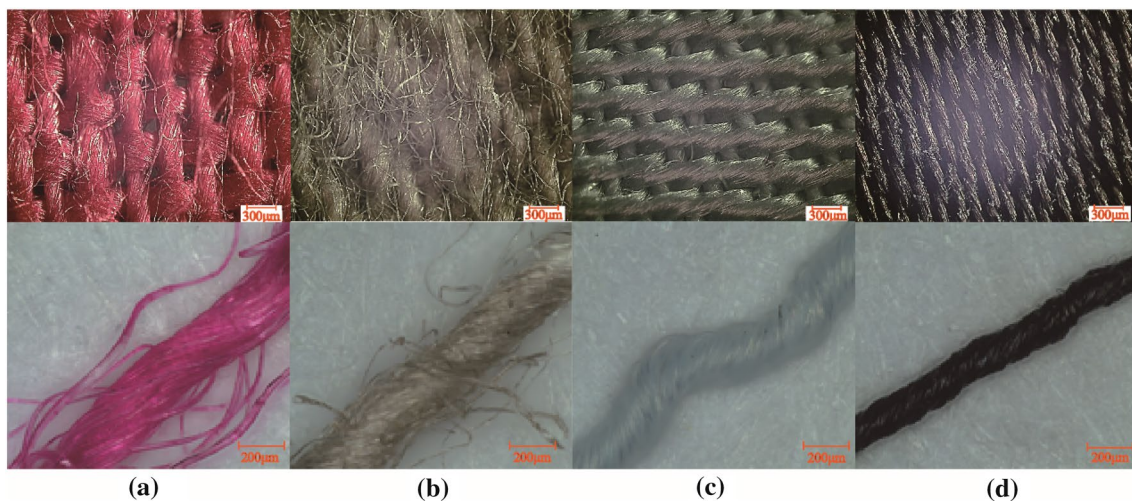


**Fig. 1** Surface microscopy images of fabric samples: **a** linen, **b** cotton, **c** polyester, and **d** silk

**Table 1** Surface properties of fabrics

	Linen	Cotton	Polyester	Silk
Structure	Plain	Plain	Twill	Twill
Component	Linen100%	Cotton100%	Polyester100%	Silk100%
Surface roughness $R_a$ ( $\mu\text{m}$ )	37.52	25.64	20.81	9.03
Diameter of single fiber ( $\mu\text{m}$ )	46.04	33.33	26.64	16.21
Diameter of one-strand fibers ( $\mu\text{m}$ )	236	205	196	132
Warp-weft density $D$ ( $10\text{ cm}^{-1}$ )	$251 \times 212$	$233 \times 256$	$294 \times 376$	$487 \times 408$
Thickness (mm)	0.36	0.35	0.32	0.34
Water absorption capacity ( $\text{mg}/\text{cm}^2$ )	23.7	18.5	13.5	21.4

**Table 2** Formulation of artificial sweat solutions

	Water	Lactic acid	Sodium chloride	Urea	pH
Composition	98%	0.1%	1.0%	0.1%	6.5

The water absorption capacity could represent the water absorption capacity of fabric and be measured according to the literatures [11, 21]. After immersion in water for 5 min, a fabric sample was vertically hung on a rod until no water dropped within 30 s. The weight of a wet sample minus the weight of a dry sample divided by the sample area was defined as the water absorption capacity.

## 2.2 Participants

Twenty healthy, 20–25 years of age (mean  $\pm$  standard deviation =  $22.1 \pm 1.7$  years), right-handed males from our college, participated in this study. All subjects were healthy and signed informed consent before the test. This study followed international ethical standards and was approved by the Ethics Committee of Xuzhou Central Hospital (No. XZXY-LJ-20210513-054).

## 2.3 Design of Fabric Wetness Levels

All tests were performed in an experimental room at 24–26 °C and 40–60% relative humidity. The formulation of artificial sweat is shown in Table 2.

Three wetness levels (dry, moist, and wet conditions) were designed in this study. In dry conditions of fabrics, there was no sweat applied to the fabric surfaces. In order to prepare the moist and wet conditions of fabric surfaces, 0.3 and 0.6 g (i.e., 8 and 16  $\text{mg}/\text{cm}^2$ ) amounts of sweat were sprayed onto the fabric surfaces. According to the method described in references [11, 22], the fabric was laid flat in a plastic bag. A graduated micropipette with a minimum volume of 0.1 ml was used to add different amounts of sweat to the fabric sample. It was positioned at a distance of approximately 5 cm perpendicular to the center of each sample. To prevent evaporation of water and ensure the even wetting of

the fabric sample, a plastic bag was sealed and conditioned for at least 24 h in the test environment after the water had distributed uniformly across the sample.

## 2.4 Friction-EEG Synchronization Measurement

To collect the friction signals of the finger and the tactile response of the brain while touching the fabrics simultaneously, a test bed was designed for the friction-EEG experiment, which is shown in Fig. 2. To maintain the stability of touching pressure and velocity and avoid body movement during touching, a passive touching method was adopted. The fabric samples were fixed on the stage of the tri-axial force sensor with double-coating tape and rubbed against the surface of the fingers which were kept still and fixed by tap on rack during the test. The movement of the touching platform was controlled by the ball screw and single-chip programming.

A tri-axial force sensor with a range of 50 N, accuracy error of 0.5%, output impedance of  $350 \pm 3\ \Omega$ , and sensitivity of 1 mV/V was fixed to the touching platform and used to record the friction and touching normal load. An acceleration with a sensitivity of 20 mV/g, a measurement range of 250 g, and a frequency of 1–10,000 Hz were fixed to the nail cap of the right index finger to obtain the vibration signals during tactile perception.

To ensure the synchronous triggering of events, a tactile trigger device was designed that consists of the tri-axial force sensor and one square-wave generator. The touching normal load detected by tri-axial force sensor was changed into an electric pulse by a square-wave generator that triggered the EEG system amplifier and marked the start of touch. In this way, the synchronization of touching action and EEG data collection could be ensured. Figure 3 shows a typical synchronization EEG and friction signals when the finger touched the linen samples under the dry condition.

A 32-channel EEG System (ANT Neuro, Hengelo, the Netherlands) was used to record EEG data in sync with the friction experiment. As shown in Fig. 4, C3, CP1, CP5, P3, CZ, PZ, C4, CP2, CP6, P4, and POZ electrodes were

**Fig. 2** Structure schematic diagram of test bed

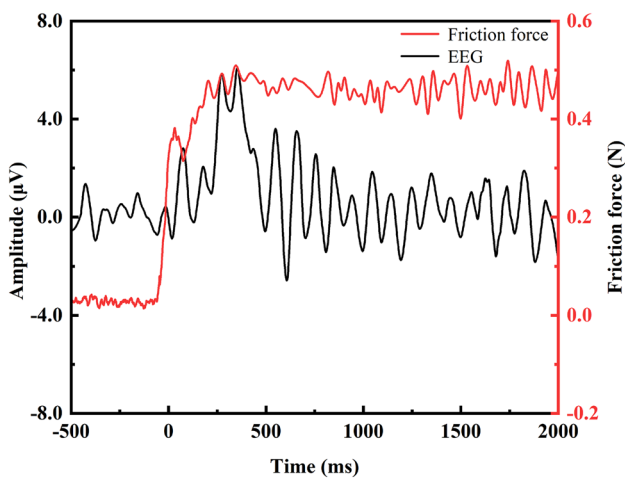
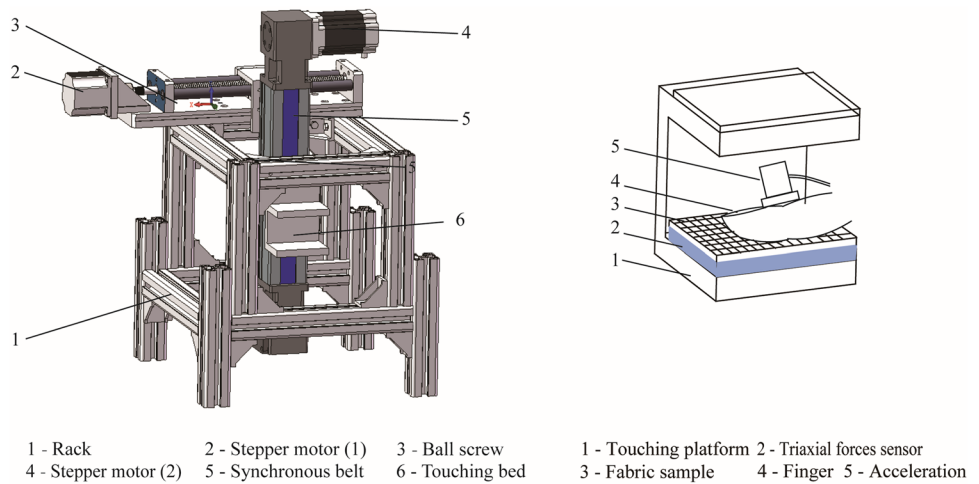


**Fig. 3** Typical synchronization EEG and friction signals

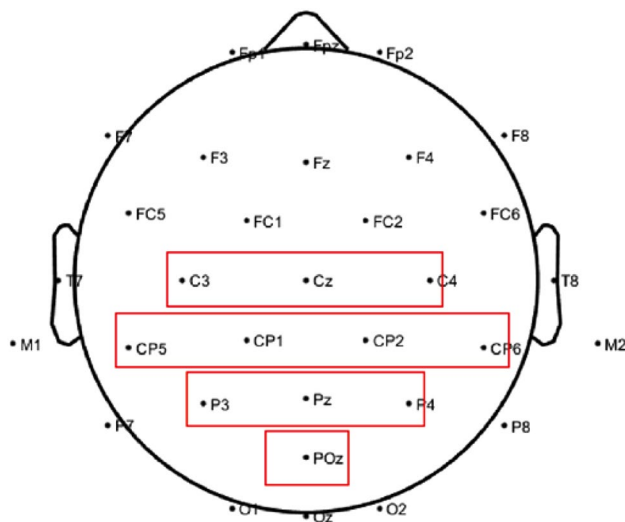


**Fig. 4** Electrode distribution pattern

chosen for further research since the parietal lobe is the area of the brain that is strongly involved in tactile sensation [23, 24].

The ERP components were evoked using an oddball paradigm. Oddball usually requires two types of stimuli simultaneously, the target and nontarget stimuli [25]. In this study, a smooth acrylic plate was chosen as the nontarget stimulus. The fabric samples under dry, moist, and wet conditions were chosen as the target stimulus. The pseudorandom sequence, which included 30 times for the target stimulation and 90 times for the nontarget stimulation, was employed. One target stimulus and one nontarget stimulus were presented in each trial. The P300 components of ERP waveform that related to the stickiness perception could only be induced when the participant actively engaged in the task of detecting the target stimuli. To ensure the concentration on the test, all subjects were asked to click the mouse button once they felt the target sample.

During the test, the subjects sat in a comfortable position and placed their arms and fingers on the rack with their ears plugged and their eyes closed. By changing the distance between the finger and the samples, the normal load can be maintained at approximately 0.5–0.8 N, which was monitored by the tri-axial force sensor. Then, the fingers were fixed by the tap. The test was carried out at a touch velocity of 15 mm/s and a distance of 30 mm for 2 s and then took 4 s to reset and exchange the samples. Each touch trial was repeated twice with 5 min of rest.

In the variable normal load test, the different touching loads (0.5, 1.0, 1.5, 2.0, and 2.5 N) were applied to subjects under the dry condition and were monitored by the tri-axial force sensor. The touching distance and velocity were 30 mm and 15 mm/s, respectively. Each touch trial was repeated three times.



## 2.5 Denoising and Feature Extraction of Vibration Signals

Since the noise from the device and environment will induce vibration, the empirical mode decomposition (EMD) method was used to remove the noise [26]. The vibration signal was decomposed into some intrinsic mode functions (IMFs) which were correlated with the no-load vibration signals. IMFs with correlation coefficients less than 0.6 were reconstructed to obtain the denoised vibration signals of touching.

Multifractal analysis is an effective statistical method for describing the dynamics of physical systems [27]. A multifractal is defined as an infinite set of singular measures over a fractal structure consisting of multiple scalar indexes. The one-dimensional time series can be divided and processed into different boxes of size  $\varepsilon$  ( $\varepsilon < 1$ ) [28]. The sum of the amplitudes of all vibration signals in the  $i$ th box of size  $\varepsilon$  is assumed to be  $S_i(\varepsilon)$ . The sum of all vibration signal amplitudes is recorded as  $\sum S_i(\varepsilon)$ , and the probability  $P_i(\varepsilon)$  is given by the following expression [29]:

$$P_i(\varepsilon) = S_i(\varepsilon) / \sum S_i(\varepsilon). \quad (1)$$

The probability measure  $P_i(\varepsilon)$  can be divided into a series of subsets, i.e., subsets of power functions that satisfy the following expression:

$$P_i(\varepsilon) = \varepsilon^\alpha, \quad (2)$$

where  $\alpha$  is the Hölder exponent. In the same subset of  $\alpha$ , the number of boxes,  $N(P_i(\varepsilon))$ , can be characterized by  $\varepsilon$ :

$$N(P_i(\varepsilon)) = \varepsilon^{-f(\alpha)}, \quad (3)$$

where  $f(\alpha)$  represents the fractal dimension of the subset of  $\alpha$ . Due to  $\alpha \in [\alpha_{\min}, \alpha_{\max}]$ ,  $f(\alpha)$  is a smooth unimodal function that is defined as the multifractal spectrum.

The shape and extension of the multifractal spectrum can provide critical details about the distributional properties of the vibration dataset. The parameter  $\Delta\alpha$  is defined as the widths of the multiple fractal spectrum, which can be obtained by the following expression:

$$\Delta\alpha = \alpha_{\max} - \alpha_{\min}. \quad (4)$$

The length of the range of fractal exponents in the vibration signal can be measured by  $\Delta\alpha$ . Figure 5 shows a typical multiple fractal spectrum of cotton samples under three conditions. The wider the range of fractal exponents is, the larger the value of  $\Delta\alpha$  and the great the fluctuation of vibration the signal [29]. In this study,  $\Delta\alpha$  of the vibration curves was calculated using the box dimension method. It represented the fluctuation of vibration signals.

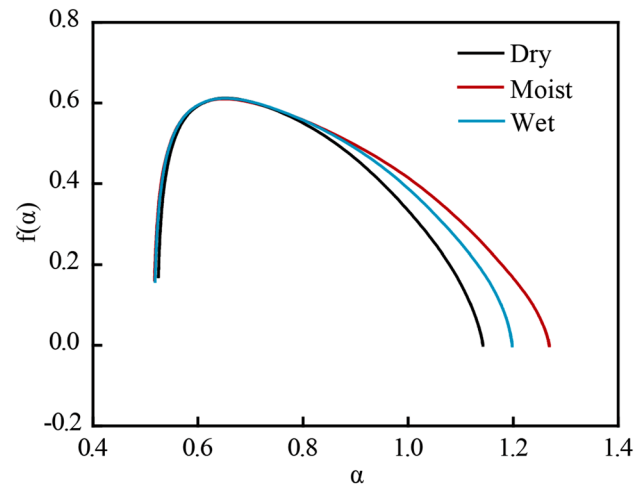


Fig. 5 A typical multiple fractal spectrum of cotton sample under three conditions

## 2.6 Processing of EEG Signals

EEGLAB, an open-source MATLAB toolbox, was used to analyze EEG data. The data were referenced to an averaged montage of ears, the bandpass was filtered between 0.5 and 40 Hz, and baseline correction was performed. The target stimulus data were then extracted for feature extraction. By superimposing and averaging the EEG data of the target stimulus in one trial, the ERP waveform was obtained. The time zero of the ERP event was defined as the time the touching began.

P300 is a positive-going electrical potential and reaches its peak at approximately 300 ms (ranging from 250 to 500 ms) after the start of external stimulation. A program in MATLAB was designed to determine the peak voltage of P300 for each electrode with a time range of 280–500 ms. The corresponding time of the peak voltage was set as the latency of P300.

## 2.7 Subjective Assessment

When the subjects touched the fabric surfaces, the main difference they felt was the stickiness of the surfaces. In this study, stickiness sensation was assessed under dry, moist, and wet fabric conditions.

A dry non-woven fabric sample was initially displayed to subjects as the reference stimulus in which perception was set as not sticky and evaluation scores for stickiness were 0. The subjects (with eyes covered and hands free) took the fabric using the left hand and rubbed the fabric surface over the forearm skin of the right hand for 10 s. Subsequently, the subjects orally expressed the stickiness feelings of the given fabric according to the reference stimulus. The fabric was presented to participants twice.

The scores ranged from 0 to 10 and were finally averaged. Higher human evaluation scores for sensations of stickiness indicated sticker feeling. The resting time between each trial was set to 2 min to avoid sensory fatigue.

### 3 Results and Discussion

#### 3.1 Correlation of Friction and Vibration Features with Stickiness Perception

Table 3 shows the stickiness perception scores (SP), coefficient of friction  $\mu$ , and  $\Delta\alpha$  of the four fabrics under different wetness levels. Pearson correlation analyses and asymptotic significance were performed to evaluate the correlation of  $\mu$  and  $\Delta\alpha$  with stickiness perception and the significant differences of data using SPSS data analysis software. The results showed that under dry and moist conditions,  $\mu$  was positively correlated with feelings of stickiness, with  $r=0.987$  and  $p=0.013$ ,  $r=0.987$  and  $p=0.013$ ;  $\Delta\alpha$  was positively correlated with feelings of stickiness, with  $r=0.987$  and  $p=0.013$ ,  $r=0.986$  and  $p=0.014$ , respectively. The result suggested that  $\mu$  and  $\Delta\alpha$  have a strong correlation with the perceived stickiness of fabrics. Under wet conditions,  $\mu$  and  $\Delta\alpha$  have no significant correlations with stickiness perception ( $r=-0.225$  and  $p=0.231$ ,  $r=-0.268$  and  $p=0.732$ ).

#### 3.2 Friction Analysis Between Skin and Fabrics Under Different Wetness Levels

As shown in Table 3, with the increase in sweat, the friction coefficient,  $\Delta\alpha$  and the stickiness perception of all fabrics showed an increasing and then decreasing trend. Figure 6 shows a schematic diagram of a finger touching the fabric surfaces under three wetness conditions. Under the dry condition, there is no hydration on the skin, and it shows minimum friction. Under the moist condition, the increase in friction is most likely due to a sweat absorption, which induces skin softening, smoothing, and reduction in interfacial shear strength and Young's modulus and therefore, the contact area increases [3, 30, 31]. In the adhesion model, the friction force increases proportionally with the nominal contact area. As the amount of sweat increases, which is especially greater than the water absorption capacity of fabrics, the friction enters the mixed lubrication regime [10, 32]. Consequently, the friction force and stickiness sensation were weakened and decreased. These results were consistent with previous reports [3, 4, 10, 30, 33–35]. The detailed discussions are as follows.

- (1) Friction analysis between skin and fabrics under dry conditions

The skin is a kind of viscoelastic material and the friction generated by the fingers sliding across the fabric mainly consists of the adhesive friction  $F_{adh}$  and the deformation friction  $F_{def}$ . It is common to describe the friction force  $F$

**Table 3** Stickiness perception, friction coefficient, and multiple fractal spectrum width of samples under different wetness levels

	Dry			Moist			Wet		
	SP	$\mu$	$\Delta\alpha$	SP	$\mu$	$\Delta\alpha$	SP	$\mu$	$\Delta\alpha$
Linen	1.4±0.5	0.68±0.04	0.58±0.05	5.5±0.3	0.82±0.06	0.69±0.06	5.1±0.6	0.80±0.06	0.67±0.06
Cotton	2.7±0.6	0.73±0.03	0.62±0.07	7.9±0.6	0.89±0.05	0.75±0.05	5.7±0.7	0.81±0.07	0.67±0.06
Polyester	4.2±0.4	0.76±0.05	0.65±0.07	9.2±0.7	0.96±0.08	0.80±0.03	5.3±0.4	0.80±0.04	0.67±0.07
Silk	5.2±0.7	0.81±0.06	0.68±0.06	6.4±0.5	0.85±0.04	0.72±0.06	5.9±0.5	0.81±0.08	0.68±0.05

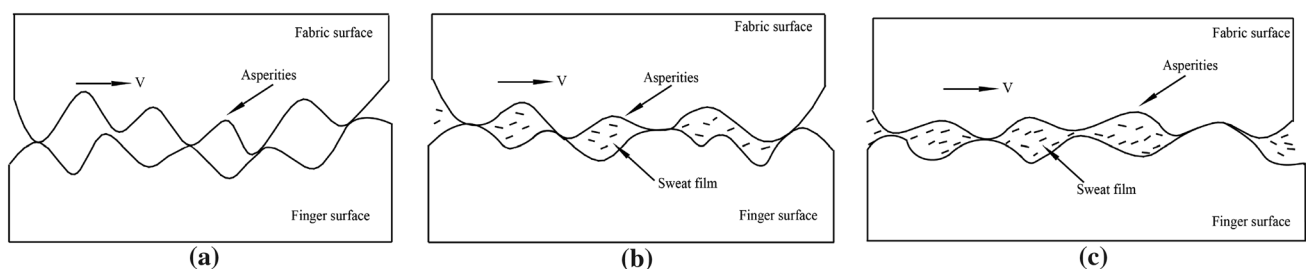


**Fig. 6** Schematic diagram of a finger touching **a** dry, **b** moist, and **c** wet fabric surfaces

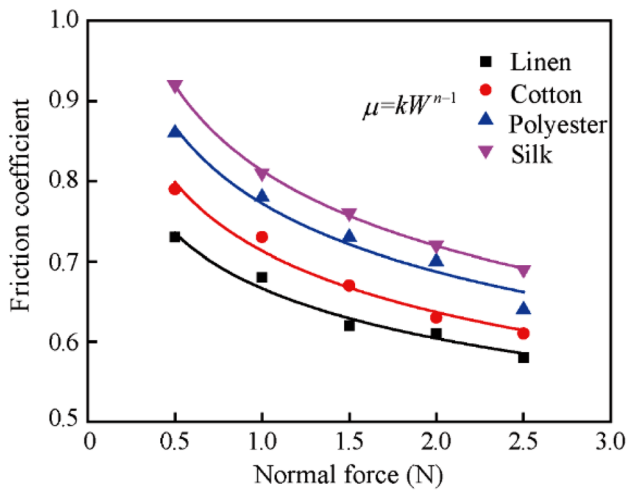


**Fig. 7** Friction coefficient as a function of applied load for fabric samples

**Table 4** Experimental and derived data of the fabric samples

	Linen	Cotton	Polyester	Silk
<i>n</i>	0.86	0.84	0.83	0.80
<i>k</i>	0.67	0.71	0.77	0.82

and the friction coefficient  $\mu$  of the skin by the following equations [30, 36]:

$$F = F_{adh} + F_{def}, \tag{5}$$

$$F_{adh} = \pi A_r = \pi \tau_0 \left(\frac{3R}{4E}\right)^{\frac{2}{3}} W^{\frac{2}{3}} + \alpha W, \tag{6}$$

$$F_{def} = \beta \left(\frac{9}{128R}\right)^{\frac{2}{3}} \left(\frac{1-\nu^2}{E}\right)^{\frac{1}{3}} W^{\frac{4}{3}}, \tag{7}$$

$$\mu = kW^{n-1}, \tag{8}$$

where  $\tau$  is the interfacial shear strength,  $A_r$  is the real contact area,  $\tau_0$  is the intrinsic interfacial shear strength,  $R$  is the radius of the sphere,  $E$  and  $\nu$  are the Young’s modulus and Poisson’s ratio of skin,  $\alpha$  is a pressure coefficient,  $W$  is the normal load, and  $\beta$  is the viscoelastic hysteresis loss fraction.  $k$  is a load-dependent friction coefficient and  $n$  is the load index. It may be seen that Eq. (6) and (7) are in the form of Eq. (8) with load indexes of 2/3 and 4/3, respectively.

In this study, the coefficients of friction as a function of the applied normal load for all samples are plotted in Fig. 7. The experimental data are fitted to Eq. (8) and the corresponding values of  $k$  and  $n$  are given in Table 4. The results showed that the friction coefficient decreased with

increasing touching load, and the value range of  $n$  was between 0.80 and 0.86, which was close to the load index of adhesive friction. The result indicated that adhesive friction plays a dominant role when skin slides over fabrics under dry conditions.

Table 3 shows that under dry conditions, the silk sample induced the strongest stickiness feeling, with the largest values of  $\mu$  and  $\Delta\alpha$ . The linen sample induced the weakest stickiness feeling with the smallest values of  $\mu$  and  $\Delta\alpha$ . The contact area is the critical factor in determining the adhesive friction. The larger the contact area is, the greater the adhesive friction is. As shown in Fig. 6a, because of the absence of sweat, the asperities of the finger directly contacted the asperities of the fabric, and the surface roughness of the fabric should be the dominant influencing factor of the contact area, which is a comprehensive characterization of weaving density, fabric structure, and fiber diameter. In the four fabrics, due to the lowest surface roughness, the highest weaving density, and the smallest signal strand fiber diameter, the silk sample has the largest contact area with the finger that induced high adhesive friction and strong stickiness perception. Meanwhile, when the finger slid over the silk surface, the high interfacial shear and adhesive friction need to be overcome which induced the great vibrating fluctuation of the fingers and the large  $\Delta\alpha$ . With increasing surface roughness, the contact area between the skin and fabric decreased, which induced decreasing friction and stickiness perception. Due to the maximum roughness, linen showed the smallest adhesive friction and  $\Delta\alpha$  and the weakest stickiness perception.

The correlations of  $\mu$ ,  $\Delta\alpha$ , and stickiness perception with surface roughness were evaluated. The results showed that surface roughness was negatively correlated with  $\mu$ ,  $\Delta\alpha$ , and stickiness perception ( $r = -0.981$  and  $p = 0.021$ ;  $r = -0.984$  and  $p = 0.023$ ;  $r = -0.982$  and  $p = 0.020$ , respectively). This demonstrated that the lower the surface roughness was, the higher the friction coefficient and the fluctuation of vibration were, and the stronger the stickiness perception was, which was consistent with the above analysis. This confirmed and proved that under the dry condition, surface roughness was one of the dominating factors that influenced the friction coefficient, vibrating fluctuation, and stickiness perceptions of fabrics.

(2) Friction analysis between skin and fabrics under moist conditions

Table 3 shows that under the moist condition, the polyester sample induced the strongest stickiness feeling, with the largest values of  $\mu$  and  $\Delta\alpha$ , and the linen sample induced the weakest stickiness feeling, with the smallest values of  $\mu$  and  $\Delta\alpha$ . As shown in Fig. 6b, sweat hydrated and softened the stratum corneum which increased the

contact area of the skin and fabric. The hydration of the stratum corneum depended on the amount of sweat retained on the surface of the fabric.

The amount of sweat that remained on the fabric surface increased due to a lower water absorption capacity of fabric, which increased the friction force and  $\Delta\alpha$  between the skin and fabric as well as strong stickiness perception [37, 38]. The polyester sample had the smallest water absorption capacity and therefore induced the largest  $\mu$  and  $\Delta\alpha$  and the strongest sticky perception. However, the linen sample had the largest water absorption capacity that caused the smallest  $\mu$  and  $\Delta\alpha$  and the weakest sticky perception.

The correlations of  $\mu$ ,  $\Delta\alpha$ , and stickiness perception with water absorption capacity were evaluated. The results showed that water absorption capacity was negatively correlated with  $\mu$ ,  $\Delta\alpha$ , and stickiness perception ( $r=-0.961$  and  $p=0.032$ ;  $r=-0.983$  and  $p=0.022$ ;  $r=-0.964$  and  $p=0.012$ , respectively). This demonstrated that the lower the water absorption capacity was, the higher the friction coefficient and the fluctuation of vibration were, and the stronger the stickiness perception was, which was consistent with the above analysis. This confirmed and proved that under the moist condition, water absorption capacity was one of the dominating factors that influenced the friction

coefficient, vibrating fluctuation, and stickiness perceptions of fabrics.

### (3) Friction analysis between skin and fabrics under the wet condition

Table 3 shows that under the wet condition, the stickiness of the four fabric samples was similar and the values of  $\mu$  and  $\Delta\alpha$  were close. Under the wet condition, the skin and fabric were saturated by water and excess water accumulated at in the interface. A layer of sweat film will be formed, acting as mixed lubrication [10, 32]. As shown in Fig. 6c, there were both sweat film and direct contact of asperities between skin and fabrics. In this case, the effect of surface roughness and water absorption capacity decreased, sweat film was one of the dominating factors, and the friction, vibration, and stickiness feelings of the four fabrics did not show significant differences.

### 3.3 EEG Analysis of Stickiness Perception Under Different Wetness Levels

Figure 8 shows the average ERP scalp maps at the time windows of 50–60 ms, 210–220 ms, 310–320 ms, and 350–360 ms of four samples under three conditions. The

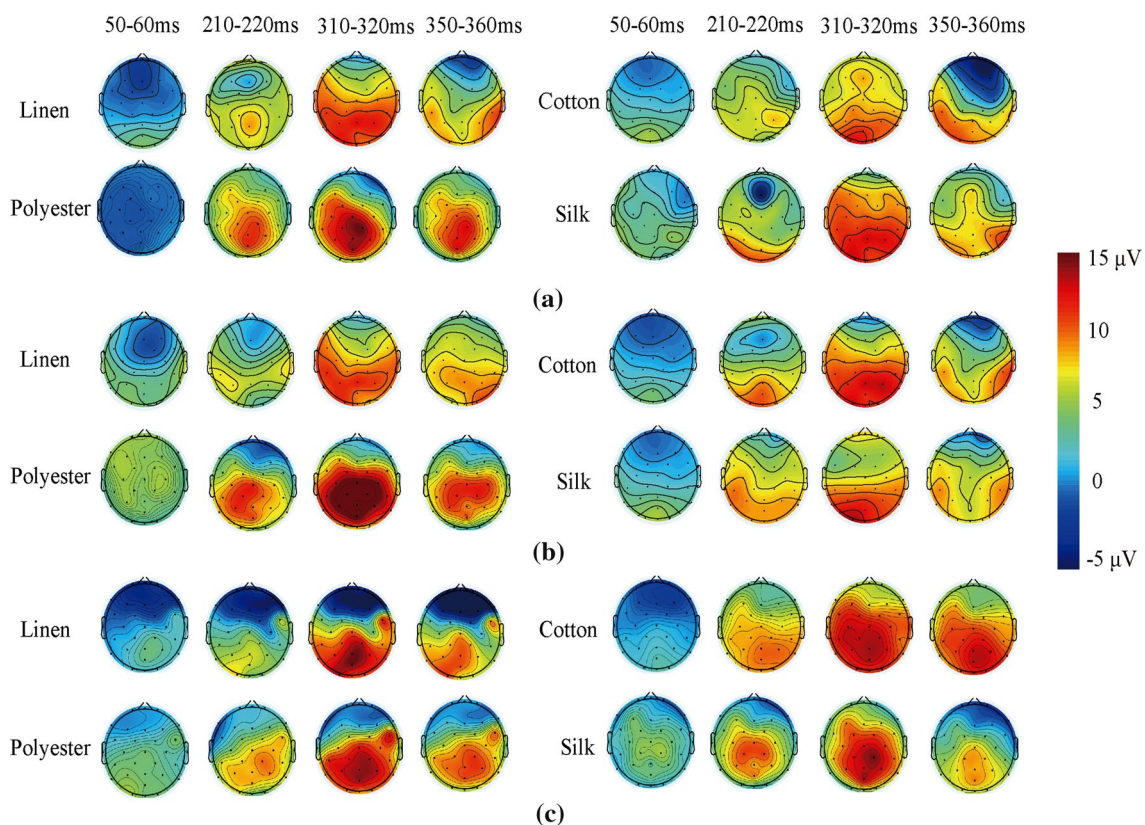


**Fig. 8** Average ERP scalp maps under **a** dry, **b** moist, and **c** wet conditions



color change from blue to red corresponded to the voltage change from low to high. It could reflect the active brain area and size. The scalp topography demonstrated that the parietal lobe and occipital lobe areas were positively activated, which was responsible for the recognition of textures [18, 21]. Our results are consistent with these studies. It also showed that under the dry condition, silk induced the largest activated brain area, while cotton induced the smallest activated brain area. Under moist conditions, polyester induced the largest activated brain area, while linen induced the smallest one. Under the wet condition, cotton induced the largest activated brain area, while linen induced the smallest activated brain area.

Figure 9 displays the average ERP waveform of the chosen electrodes. Table 5 summarizes the mean latency and amplitude of P300 components of ERP. The scalp topography and ERP waveform indicated that with the processing of touching, the ERP amplitude of the four fabrics gradually increased and reached to the maximum at the P300 component, followed by a decrease.

The P300 component is a typical endogenous component stimulated during the decision-making process and can reflect basic cognitive processes. The difference between the mean pre-stimulus baseline voltage and the ERP waveform's largest positive-going peak within a time window is known as the P300 amplitude [39]. According to references [15, 40], the P300 amplitude is proportional to the number of attentional resources involved in processing the given stimulus. The time between the onset of the stimulus and peak-positive amplitude during a time window is known as the P300 latency. It reflects the speed of volunteers' judgment for the fabric surface texture and is correlated with the difficulty of the task [41]. Therefore, the P300 component was used as an electrophysiological representation of the stickiness perception of fabric.

The results showed that under different wetness conditions, the P300 latency evoked by the four fabrics had no significant differences, indicating that the subjective judgment

**Table 5** Latency and amplitude of P300 components of ERP

Samples	Latency (ms)/ Amplitude ( $\mu$ V)		
	Dry	Moist	Wet
Linen	311 <sup>a</sup> /9.3 <sup>a</sup>	325 <sup>a</sup> /6.5 <sup>a</sup>	323 <sup>a</sup> /6.0 <sup>a</sup>
Cotton	306 <sup>a</sup> /6.5 <sup>b</sup>	321 <sup>a</sup> /9.8 <sup>b</sup>	319 <sup>a</sup> /7.2 <sup>a</sup>
Polyester	310 <sup>a</sup> /8.0 <sup>c</sup>	311 <sup>a</sup> /11.1 <sup>c</sup>	314 <sup>a</sup> /6.3 <sup>a</sup>
Silk	300 <sup>a</sup> /10.4 <sup>d</sup>	318 <sup>a</sup> /8.2 <sup>d</sup>	317 <sup>a</sup> /6.8 <sup>a</sup>

Means marked with different letters in the same column are significantly different from each other, and means marked with the same letter are not significantly different from each other ( $P < 0.05$ )

speed of the fabric stickiness was almost the same. Under the dry condition, silk and linen both induced the larger P300 amplitudes, suggesting that fabrics with high surface friction and surface roughness both need a large amount of attention resources during stickiness perception. The high surface roughness induced the large contact stress of skin, and the high friction induced the large deformation and vibration of skin. These mechanical stimulations stimulated the sensory receptors of skin, leading to large amounts of attention processing in the sensorial judgments of stickiness.

Under the wet condition, there were no significant differences in P300 amplitudes of the four fabrics, indicating that the attentional resources in the stickiness perception judgment were almost the same. Under the wet condition, skin is saturated by water, and excess water accumulates at the interface. According to Table 3, the friction coefficients of the three fabrics and the widths of the multiple fractal spectra were almost the same, resulting in the similar mechanical stimulation simulating the sensory receptors of skin. Therefore, the attentional resources in the stickiness perception judgment were almost the same.

Under the moist condition, the order of P300 amplitude and activated brain area was polyester > cotton > silk > linen. Correlation analysis showed that water absorption capacity was negatively correlated with P300 amplitude with

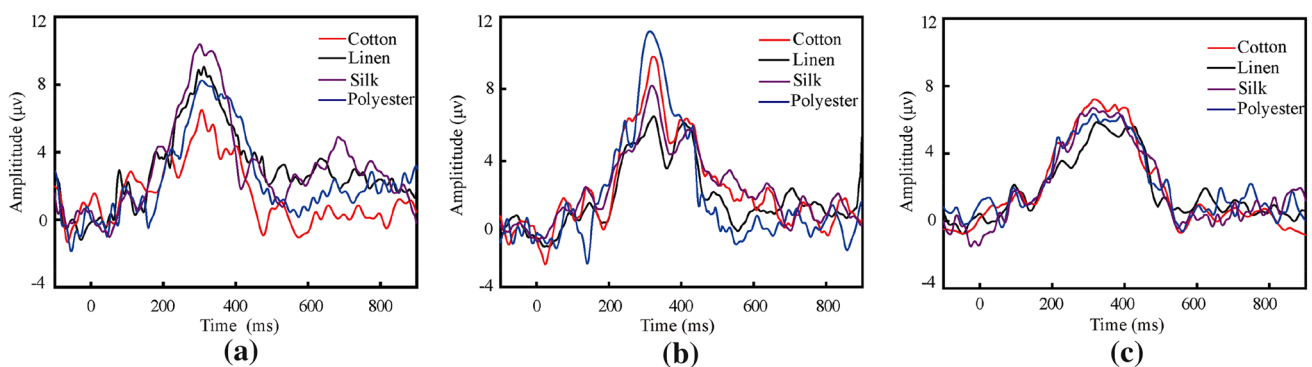


**Fig. 9** Average ERP waveform of four samples under **a** dry, **b** moist, and **c** wet conditions

$r = -0.942$  and  $p = 0.031$ . P300 amplitudes were positively correlated with feelings of stickiness,  $\mu$ , and  $\Delta\alpha$  with  $r = 0.979$  and  $p = 0.011$ ,  $r = 0.963$  and  $p = 0.012$ ,  $r = 0.973$  and  $p = 0.008$ , respectively. This result indicated that the P300 amplitude had a strong correlation with the perceived stickiness of fabrics. Fabric surfaces with low water absorption capacity and high friction coefficient need large attentional resources in the stickiness perception judgment. During the stickiness sensation of fabrics, the friction and vibration characteristics of fingers are significantly correlated with the tactile EEG signal, namely, the mechanical stimulation of the tactile receptor is associated with the brain's cognition.

## 4 Conclusion

This study systematically studied and quantitatively characterized the stickiness perception of fabrics based on a subjective evaluation, fabric features, surface friction and vibration, and the neurophysiological response of the brain. The conclusions are as follows.

For all fabric samples, the coefficient of friction decreased with increasing applied normal load, indicating that skin adhesive friction played a dominant role when skin slid over fabrics under dry fabric conditions.

With the increase in sweat, the friction coefficient,  $\Delta\alpha$ , and the stickiness perception of all fabrics increased and then decreased.

Under dry and moist conditions, the surface roughness and water absorption capacity of fabric were the dominating factors that influenced the friction coefficient, vibrating fluctuation, and stickiness perception of fabrics, respectively. Under the wet condition, due to the layer of sweat film acting as mixed lubrication, there were no significant differences in friction, vibration, and stickiness of the four fabrics.

The parietal lobe and occipital lobe were positively activated and involved in the stickiness perceptions of fabric. Under the moist condition, the P300 amplitude correlates with the water absorption capacity of the fabric. Fabrics with low water absorption capacity and high friction coefficient tended to excite a high P300 peak and large activated brain area.

The features of the coefficient of friction,  $\Delta\alpha$ , and P300 amplitude have strong correlations with the perceived stickiness of fabrics. The friction and vibration characteristics of fingers are significantly correlated with the tactile EEG signal.

As the study object of tactile sensation is human, there are many individual factors affecting tactile sensation, including age, gender, personal experience, attention, and fingerprint characteristics of the subjects. This study has unified the age, gender, and educational background of the subjects,

and further studies can be carried out on the influence of individual differences on tactile sensation.

**Acknowledgements** The authors acknowledge financial support from the National Natural Science Foundation of China No. 51875566 and A Project Funded by the Priority Academic Program Development of Jiangsu Higher Education Institutions.

**Author Contributions** All authors contributed to the study conception and design. XF wrote the main manuscript text and MZ prepared the samples. Prof. WT provided guidance on the content of the article. CT and YP reviewed the manuscript text.

**Funding** This study was funded by the National Natural Science Foundation of China No. 51875566 and A Project Funded by the Priority Academic Program Development of Jiangsu Higher Education Institutions.

**Data Availability** Data are available on request.

## Declarations

**Competing interests** The authors declare no competing interests.

**Disclosures** Xingxing Fang, Wei Tang, Chaoquan Tang, Meimei Zhang, and Yuxing Peng declare that they have no known competing financial interests to disclose or personal relationships that could have appeared to influence the work reported in this paper.

## References

- Jiang, R., Wang, Y.: Research progress of stickiness perception of human body in dressing. *J Text. Res.* **40**, 177–184 (2019). <https://doi.org/10.13475/j.fzxb.20180702008>
- Lou, L., Ji, F., Qiu, Y.: Simulating adhesion of wet fabrics to water: Surface tension-based theoretical model and experimental verification. *Text. Res. J.* **85**, 1987–1998 (2015). <https://doi.org/10.1177/0040517515580531>
- Gerhardt, L.C., Strässle, V., Lenz, A., Spencer, N.D., Derler, S.: Influence of epidermal hydration on the friction of human skin against textiles. *J. R. Soc. Interface.* **5**, 1317–1328 (2008). <https://doi.org/10.1098/rsif.2008.0034>
- Maggie, K.P., Chau, K.H., Kan, C.W., Fan, Jtu: Magnitude estimation approach for assessing stickiness sensation perceived in wet fabrics. *Fibers Polym.* **19**, 2418–2430 (2018). <https://doi.org/10.1007/s12221-018-8626-9>
- Johnson, K.: Neural mechanisms of tactual form and texture perception. *Annu. Rev. Neurosci.* **15**, 227–250 (1992). <https://doi.org/10.1146/annurev.neuro.15.1.227>
- Bodegård, A., Ledberg, A., Geyer, S., Naito, E., Zilles, K., Roland, P.E.: Object shape differences reflected by somatosensory cortical activation. *J. Neurosci.* **20**, RC51 (2000). <https://doi.org/10.1523/jneurosci.20-01-j0004.2000>
- Amaied, E., Vargiolu, R., Bergheau, J.M., Zahouani, H.: Aging effect on tactile perception: Experimental and modelling studies. *Wear* **332–333**, 715–724 (2015). <https://doi.org/10.1016/j.wear.2015.02.030>
- Renganathan, P., Schwartz, C.J.: Investigation of human perception of tactile graphics and its dependence on fundamental friction mechanisms. *Wear.* **476**, 203729 (2021). <https://doi.org/10.1016/j.wear.2021.203729>
- Derler, S., Gerhardt, L.C.: Tribology of skin: Review and analysis of experimental results for the friction coefficient of human

- skin. *Tribol. Lett.* **45**, 1–27 (2012). <https://doi.org/10.1007/s11249-011-9854-y>
10. Tomlinson, S.E., Lewis, R., Liu, X., Texier, C., Carré, M.J.: Understanding the friction mechanisms between the human finger and flat contacting surfaces in moist conditions. *Tribol. Lett.* **41**, 283–294 (2011). <https://doi.org/10.1007/s11249-010-9709-y>
  11. Jiang, R., Wang, Y.: Study of the human stickiness perception of wet fabric on the volar forearm via two contact modes: friction and adhesion-separation. *Perception* **49**, 1311–1332 (2020). <https://doi.org/10.1177/0301006620976992>
  12. Zhang, Z., Tang, X., Li, J., Yang, W.: The effect of dynamic friction with wet fabrics on skin wetness perception. *Int. J. Occup. Saf. Ergon.* **26**, 370–383 (2020). <https://doi.org/10.1080/10803548.2018.1453023>
  13. Mougou, A., Thonnard, J.L., Mouraux, A.: EEG frequency tagging to explore the cortical activity related to the tactile exploration of natural textures. *Sci. Rep.* (2016). <https://doi.org/10.1038/srep20738>
  14. Muñoz, F., Reales, J.M., Sebastián, M.Á., Ballesteros, S.: An electrophysiological study of haptic roughness: Effects of levels of texture and stimulus uncertainty in the P300. *Brain Res.* **1562**, 59–68 (2014). <https://doi.org/10.1016/j.brainres.2014.03.013>
  15. Tang, W., Zhang, M., Chen, G., Liu, R., Peng, Y., Chen, S., Shi, Y., Hu, C., Bai, S.: Investigation of tactile perception evoked by ridged texture using ERP and non-linear methods. *Front. Neurosci.* (2021). <https://doi.org/10.3389/fnins.2021.676837>
  16. Inui, K., Wang, X., Tamura, Y., Kaneoke, Y., Kakigi, R.: Serial processing in the human somatosensory system. *Cereb Cortex.* **14**, 851–857 (2004). <https://doi.org/10.1093/cercor/bhh043>
  17. Adhikari, B.M., Sathian, K., Epstein, C.M., Lamichhane, B., Dhamala, M.: Oscillatory activity in neocortical networks during tactile discrimination near the limit of spatial acuity. *Neuroimage* **91**, 300–310 (2014). <https://doi.org/10.1016/j.neuroimage.2014.01.007>
  18. Chen, S., Ge, S.: Experimental research on the tactile perception from fingertip skin friction. *Wear* **376–377**, 305–314 (2017). <https://doi.org/10.1016/j.wear.2016.11.014>
  19. Tang, W., Lu, X., Chen, S., Ge, S., Jing, X., Wang, X., Liu, R., Zhu, H.: Tactile perception of skin: research on late positive component of event-related potentials evoked by friction. *J. Text. Inst.* **111**, 623–629 (2020). <https://doi.org/10.1080/00405000.2019.1661067>
  20. Camillieri, B., Bueno, M.A., Fabre, M., Juan, B., Lemaire-Semail, B., Mouchnino, L.: From finger friction and induced vibrations to brain activation: Tactile comparison between real and virtual textile fabrics. *Tribol. Int.* **126**, 283–296 (2018). <https://doi.org/10.1016/j.triboint.2018.05.031>
  21. Tang, K.P.M., Kan, C.W., Fan, J.T.: Psychophysical measurement of wet and clingy sensation of fabrics by the volar forearm test. *J. Sens. Stud.* **30**, 329–347 (2015). <https://doi.org/10.1111/joss.12161>
  22. Raccuglia, M., Hodder, S., Havenith, G.: Human wetness perception in relation to textile water absorption parameters under static skin contact. *Text. Res. J.* **87**, 2449–2463 (2017). <https://doi.org/10.1177/0040517516671127>
  23. Gottlieb, J.: From thought to action: The parietal cortex as a bridge between perception, action, and cognition. *Neuron* **53**, 9–16 (2007). <https://doi.org/10.1016/j.neuron.2006.12.009>
  24. Chen, Y.S., Chen, H.L., Lu, C.H., Chen, M.H., Chou, K.H., Tsai, N.W., Yu, C.C., Chiang, P.L., Lin, W.C.: Reduced lateral occipital gray matter volume is associated with physical frailty and cognitive impairment in Parkinson's disease. *Eur. Radiol.* **29**, 2659–2668 (2019). <https://doi.org/10.1007/s00330-018-5855-7>
  25. Teodorescu, M., Rahnejat, H.: Nano-scale contact model for microfiber tip attachment, detachment and friction. *2008 Proc STLE/ASME Int J Tribol Conf IJTC* **2008**, 83–85 (2009). <https://doi.org/10.1115/ijtc2008-71220>
  26. Li, C., Zhang, T., Zang, X., Zhao, Z., Fang, L., Zhao, N.: Void fraction measurement based on flow noise decoupling and differential pressure. *IEEE Trans. Instrum. Meas.* **71**, 1–12 (2022). <https://doi.org/10.1109/TIM.2022.3151153>
  27. Albuquerque, E.L., Cottam, M.G.: Plasmon-polaritons in quasiperiodic structures. *Polaritons Period: Quasiperiodic Struct.* (2004). <https://doi.org/10.1016/b978-044451627-5/50006-7>
  28. Li, J., Zhang, X., Tang, J., Cai, J., Liu, X.: Audio magnetotelluric signal-noise identification and separation based on multifractal spectrum and matching pursuit. *Fractals* **27**, 1940007 (2019). <https://doi.org/10.1142/S0218348X19400073>
  29. Li, G., Huang, Y., Lin, Y., Pan, X.: Multifractal analysis of frictional vibration in the running-in process. *Tribol. Trans.* **56**, 284–289 (2013). <https://doi.org/10.1080/10402004.2012.750023>
  30. Adams, M.J., Briscoe, B.J., Johnson, S.A.: Friction and lubrication of human skin. *Tribol. Lett.* **26**, 239–253 (2007). <https://doi.org/10.1007/s11249-007-9206-0>
  31. Derler, S., Rotaru, G.M., Ke, W., Issawi-Frischknecht, L.E., Kellenberger, P., Scheel-Sailer, A., Rossi, R.M.: Microscopic contact area and friction between medical textiles and skin. *J. Mech. Behav. Biomed. Mater.* **38**, 114–125 (2014). <https://doi.org/10.1016/j.jmbbm.2014.06.014>
  32. Derler, S., Gerhardt, L.C., Lenz, A., Bertaux, E., Hadad, M.: Friction of human skin against smooth and rough glass as a function of the contact pressure. *Tribol. Int.* **42**, 1565–1574 (2009). <https://doi.org/10.1016/j.triboint.2008.11.009>
  33. André, T., Lefèvre, P., Thonnard, J.L.: A continuous measure of fingertip friction during precision grip. *J. Neurosci. Methods.* **179**, 224–229 (2009). <https://doi.org/10.1016/j.jneumeth.2009.01.031>
  34. Nonomura, Y., Fujii, T., Arashi, Y., Miura, T., Maeno, T., Tashiro, K., Kamikawa, Y., Monchi, R.: Tactile impression and friction of water on human skin. *Colloids Surfaces B Biointerfaces.* **69**, 264–267 (2009). <https://doi.org/10.1016/j.colsurfb.2008.11.024>
  35. Raccuglia, M., Pistak, K., Heyde, C., Qu, J., Mao, N., Hodder, S., Havenith, G.: Human wetness perception of fabrics under dynamic skin contact. *Text. Res. J.* **88**, 2155–2168 (2018). <https://doi.org/10.1177/0040517517716905>
  36. Wolfram, L.J.: Friction of skin. *J. Soc. Cosmet. Chem.* **34**, 465–476 (1983)
  37. Sivamani, R.K., Maibach, H.I.: Tribology of skin. *P. I. Mech. Eng. J-J. Eng.* **220**, 729–737 (2006). <https://doi.org/10.1243/13506501JET85>
  38. Hendriks, C.P., Franklin, S.E.: Influence of surface roughness, material and climate conditions on the friction of human skin. *Tribol. Lett.* **37**, 361–373 (2010). <https://doi.org/10.1007/s11249-009-9530-7>
  39. Polich, J.: Updating P300: An integrative theory of P3a and P3b. *Clin. Neurophysiol.* **118**, 2128–2148 (2007). <https://doi.org/10.1016/j.clinph.2007.04.019>
  40. Gray, H.M., Ambady, N., Lowenthal, W.T., Deldin, P.: P300 as an index of attention to self-relevant stimuli. *J. Exp. Soc. Psychol.* **40**, 216–224 (2004). [https://doi.org/10.1016/S0022-1031\(03\)00092-1](https://doi.org/10.1016/S0022-1031(03)00092-1)
  41. Donchin, E., Isreal, J.B.: Event-related potentials and psychological theory. *Prog. Brain Res.* **54**, 697–715 (1980). [https://doi.org/10.1016/S0079-6123\(08\)61692-1](https://doi.org/10.1016/S0079-6123(08)61692-1)

**Publisher's Note** Springer Nature remains neutral with regard to jurisdictional claims in published maps and institutional affiliations.

Springer Nature or its licensor (e.g. a society or other partner) holds exclusive rights to this article under a publishing agreement with the author(s) or other rightsholder(s); author self-archiving of the accepted manuscript version of this article is solely governed by the terms of such publishing agreement and applicable law.